Chemical Engineering Greetings to prof. Eliseo Ranzi

on occasion of his 65th birthday

Editor: *prof. Mario Dente*

ISBN 0390-2358

CFD SIMULATION OF A MIXING-SENSITIVE REACTION IN UNBAFFLED VESSELS

F. Grisafi , F. Scargiali , A. Brucato
Dip. di Ingegneria Chimica dei Processi e dei Materiali; Università di Palermo

Stirred tanks are widely used in the process industry, often to carry out complex chemical reactions. In many of such cases the perfect mixing hypothesis is not applicable for modelling purposes, and more detailed modelling approaches are required in order to accurately describe the reactor behaviour. In this work a fully predictive modelling approach, based on Computational Fluid Dynamics, is developed. Model predictions are compared with original experimental data obtained in un unbaffled stirred vessel with a parallel-competitive, mixing sensitive reaction scheme. Notably, satisfactory results are obtained at all injection rates with no recourse to *micro-mixing* model, thus confirming the major role played by *macro-mixing* in the investigated system.

1. INTRODUCTION

Due to their importance in the process industry, stirred reactors have been for decades the subject of investigations. In many cases the modelling approaches developed were aimed at setting up correlations among spatially averaged (lumped) parameters, such as average temperature and reagents concentration (perfect mixing assumption). When this did not lead to acceptable results, simple heuristic flow models were devised to try to simulate the departure of real behaviour from perfect mixing (Van De Vusse, 1962; Khang & Levenspiel, 1976).

In order to avoid the limitations associated with the lumping process and to build-up generally applicable models, distributed parameter modelling approaches of mixed reactors have been developed (Middleton *et al.*, 1986; Bakker & van den Hakker, 1994, 1996; Brucato *et al.* 2000, Baldyga & Makowski, 2004; Akiti & Armenante, 2004). All of these models are based on the actual vessel hydrodynamics and take advantage of the continuing decrease of computing costs in conjunction with the development of commercial codes for computational fluid dynamics (CFD). In some of the above works, micromixing models have been included in the CFD calculations in order to account for the mixing phenomena unresolved by the computational grid adopted.

In the present work, CFD simulations of mixing sensitive reactions are carried out and compared with original experimental data. In particular a semi-batch stirred reactor where a pair of parallel-competitive reactions takes place, was simulated:

$$\text{Reaction 1} \qquad \mathrm{A + B} \xrightarrow{k_1} \text{Prod.1}$$

$$\text{Reaction 2} \qquad \mathrm{A + C} \xrightarrow{k_2} \text{Prod. 2}$$

where k_1 and k_2 (with $k_1 >> k_2$) are the second order constants of the two reaction kinetics. The reaction scheme here employed is the same as that previously adopted by Brucato *et al.* (2000). In that case the experimentation concerned a *baffled* stirred batch reactor and an instantaneous addiction of the common reagent (*A*). Results showed that there was no need to resort to micro-mixing models to match simulation and experiment, despite the same reaction scheme had been used in the past to validate micro-mixing models (e.g. Rice & Baud, 1990; Thorma *et al.*, 1992; Baldyga *et al.*, 1997, Baldyga & Makowski, 2004). In the present work, apart from the unbaffling that results into lower turbulence levels, reactant A injection was either slow or very slow, in order to test whether micromixing phenomena became important under such conditions.

2. EXPERIMENTAL WORK

The reactive system employed in this work consists of two fast parallel-competitive reactions: the precipitation reaction of cupric hydroxide and the alkaline hydrolysis of ethyl chloroacetate (Brucato *et al.,* 2000):

$$\begin{array}{ccccccccc} \mathrm{NaOH} & + & \tfrac{1}{2}\mathrm{CuSO_4} & \xrightarrow{k_1} & \tfrac{1}{2}\mathrm{Cu(OH)_2}\downarrow & + & \tfrac{1}{2}\mathrm{Na_2SO_4} & & (1) \\ (A) & & (B) & & (R1) & & (R2) & & \end{array}$$

$$\begin{array}{ccccccccc} \mathrm{NaOH} & + & \mathrm{CH_2ClCOOC_2H_5} & \xrightarrow{k_2} & \mathrm{ClCH_2COONa} & + & \mathrm{C_2H_5OH} & & (2) \\ (A) & & (C) & & (S1) & & (S2) & & \end{array}$$

Both reactions are characterized by second order kinetics but the former is much faster than the latter. As a matter of fact, at 20 °C, the value of k_1 is of the order of 10^7 $m^3mol^{-1}s^{-1}$ while the kinetic constant k_2 is equal to 0.023 $m^3mol^{-1}s^{-1}$ (Bourne & Yu, 1991). This implies that to all practical purposes reaction (1) can be considered as instantaneous with respect to the reaction (2) when reactant concentrations are of the same order of magnitude. The reaction scheme here employed slightly differs from the well known reaction scheme employed in a number of previous investigations (*e.g.* Bourne & Yu, 1991; Baldyga & Makowski, 2004; Akiti & Armenante, 2004), where the first reaction was the acid-base neutralization of $NaOH$ with HCl. A similar reaction scheme was used by Baldyga & Bourne (1990) who utilised Fe^{3+} ions instead of Cu^{++}. In this work, the recourse to cupric ions leads to easier concentration measurements, as these could be made by direct colorimetry, taking advantage of the strong blue coloration of cupric ions. At the same time the problems related to the stoichiometric complexity of the reaction between Fe^{3+} and OH^-, due to the stability the over-hydroxylated ionic species (Cotton & Wilkinson, 1988), were avoided.

2.1 Experimental apparatus

The experimental apparatus consisted of a cylindrical unbaffled vessel with the inner diameter equal to 0.19 m closed by a flat lid and stirred by a standard radial impeller (Rushton turbine). The geometrical details of the agitation system are reported in Fig. 1. In all cases an aqueous solution with an initial concentration of 11.5 mol/lt $CuSO_4$ premixed with 21 mol/lt of $CH_2ClCOOC_2H_5$ was utilized. The operating temperature was always kept at 20 °C.

After stable fluid dynamic conditions were achieved, a concentrated solution of $NaOH$ (amounting to about 1/50 of the tank volume) was fed through a needle (0.5 mm diameter, in order to prevent back-mixing inside the feed tube) placed at an axial position of 3 cm above vessel bottom. Injection times spanned from few hundreds to several thousand seconds. The apparatus utilised to inject the concentrated $NaOH$ solution consisted of a small reservoir which was suitably filled with the solution and pressurised with air. The reservoir was connected to the needle with a PVC capillary tube (ID 0.8 mm) through an outlet valve. The injection flow rate was regulated by varying the pressure inside the reservoir and the tube's length, which was responsible for the majority of pressure drop. In this way a constant flow rate of the co-reactant was obtained.

At the end of each injection the total amount of reactant A introduced in the system was such that, in absence of chemical reactions, an average concentration of 21 molt/lt would have been attained. This implies that the amount of A fed would have been just sufficient to digest only one of the two premixed co-reactants B and C. The final concentration of reactants, when all the reactant A had disappeared, was assessed by measuring the concentration of un-reacted $CuSO_4$. The selectivity *versus* reaction 2 was finally computed as follows:

$$Sel = \frac{[C]_{init} - [C]_{final}}{[C]_{init}} \equiv \frac{[B]_{final}}{[B]_{init}} \qquad (3)$$

It is important to observe that, in the case of perfect mixing, the final selectivity expected in all investigated cases would have been of the order of 10^{-8}.

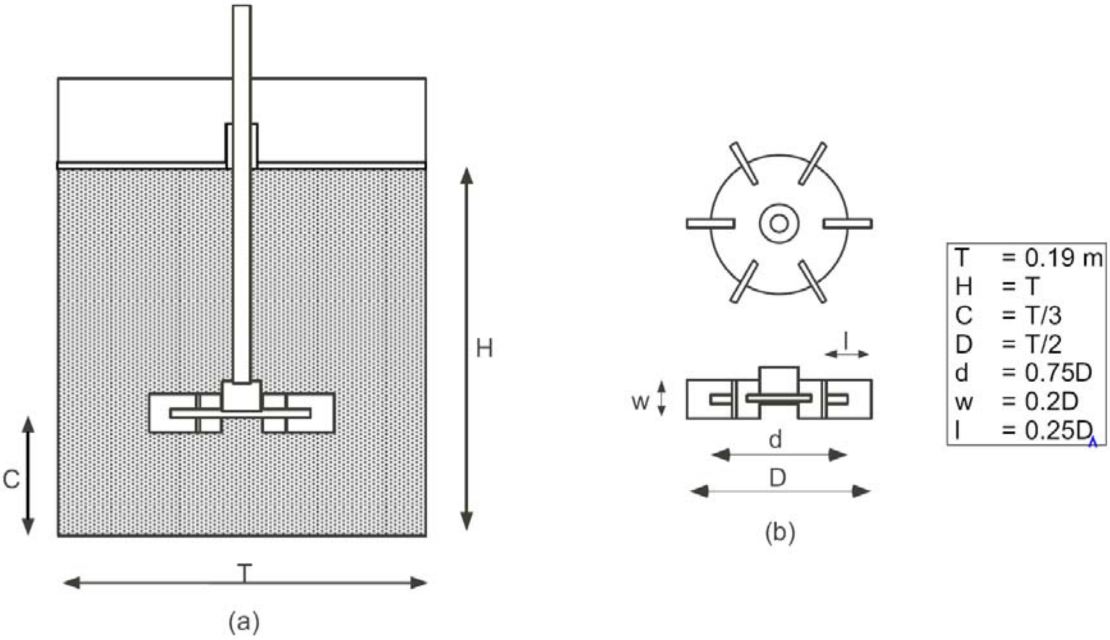

Fig. 1. Unbaffled stirred vessel employed for the experimentation

3. CFD MODELLING

The CFD modelling of the reactive process was performed in two separate steps. The pre-release flow field inside the vessel was simulated first. In the second step, while maintaining the same flow field, the three dimensional concentration dynamics of reactants was simulated until reactant A had completely disappeared from the system. Both simulations steps were carried out with the help of a commercial CFD code (STAR-CD release 3.22 by Adapco).

All simulations were performed in the impeller reference frame. With this choice it was possible to carry out steady-state flow field calculations. The system geometry also allowed considering only one sixth of the entire volume (a 60 degrees cylindrical portion). The computational domain was discretised in 42×72×12 ($r \times z \times \theta$) cells on a cylindrical reference frame. A differential Reynolds Stress second order closure was adopted for turbulence modelling, while the “SIMPLE” algorithm was adopted for the pressure-velocity coupling. The simulated flow-field was found to be dominated by tangential velocities as expected. A double loop flow pattern, similar (though weaker) to that exhibited by baffled vessels could be observed on vertical planes.

The reactive process simulations were performed for all experimental conditions starting from the corresponding steady state flow field. In this case double precision and the *QUICK* discretization scheme were adopted in order to minimise numerical diffusion problems. Due to the low concentration of reactants their presence did not significantly affect the flow field, therefore they were considered as passive scalars. The injection of reactant *A* was simulated *via* suitable source terms in the cells corresponding to the injection point.

As regards the reaction kinetics, the two reactions were treated in different ways. Reaction 1 was considered instantaneous, *i.e.* species *A* and *B* were not allowed to co-exist into the same cell. The simulation strategy for the fast reaction consisted of checking the concentrations of reactants *A* and *B* at the beginning of each time step and updating them in such a way that the limiting one disappeared while the concentration of the other was decreased according to reaction 1 stoichiometry. It is worth noting that, in each time step, there were locations in the reactor volume where reactant *A* was in excess with respect to *B* (reaction 1). In such locations the disappearance of *B* due to reaction 1 left in the same cell species *A* and *C,* that were therefore allowed to react according to reaction 2. This fact was simulated by properly setting the source terms in the transport equations of the reactants *A* and *C* according to the relevant reaction kinetics.

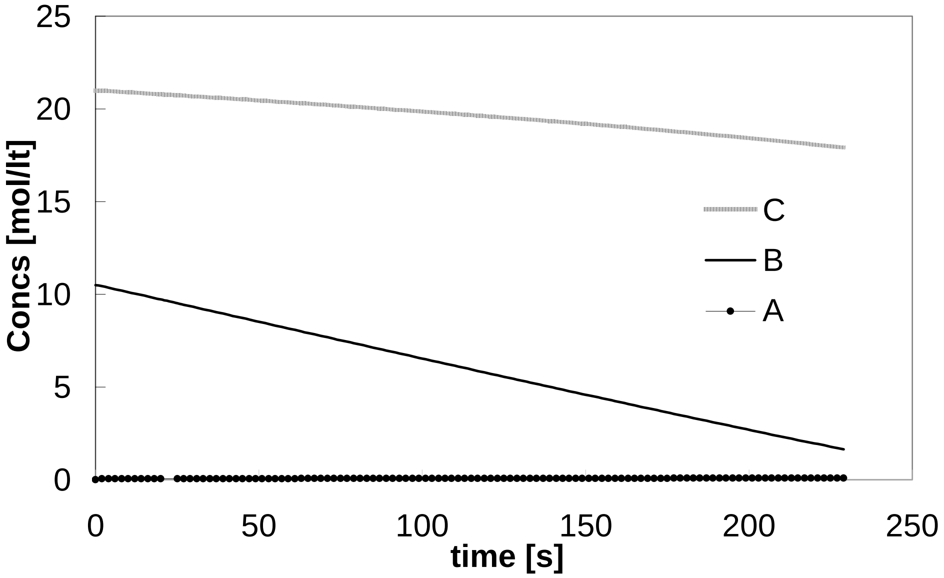

Fig. 2: Dynamics of reactant volume averaged concentrations (simulation with T_{inj}=230 s, 400 rpm).

Typical simulation results are shown in Fig. 2, in terms of average concentration dynamics of all reactants. The simulation pertains to the case of injection time equal to 230 s and agitation speed of 400 rpm. The observation of Fig. 2 indicates that the average concentrations of reactants *B* and *C* varies almost linearly with time while the concentration of co-reactant *A* is practically always close to zero.

The CPU time required to perform this simulation on a PC equipped with a Pentium dual core running at 3.2 GHz was 180 hours. The extrapolation of CPU time requirements to simulate the longest injection duration (T_{inj}=3445 s) would therefore amount to more than 1900 hours which is obviously unpractical.

In order to make the simulations affordable also for long injections times, a computational technique which speeds-up concentration dynamics calculations was set up. It is possible to define an *average reaction rate* $<r_i>$ for each reactant as follows:

$$\langle r_i \rangle = \frac{\langle C_i \rangle_{t+dt} - \langle C_i \rangle_t}{dt} \tag{4}$$

where $<C_i>_{t+dt}$ and $<C_i>_t$ are the average concentrations of reactant *"i"* (over the reactor volume) at the generic time $t + dt$ and t respectively. Analysis of the average concentration trends reported for all reactants in Fig. 2 indicates that the average reaction rates tend to become constant few seconds after the injection start. This observation makes it possible to extrapolate the average concentration of reactants B and C over a macro time interval Δt much larger than the integration time step, by simply assuming:

$$\langle C_i \rangle_{t+\Delta t} = \langle C_i \rangle_t + \langle r_i \rangle_t \cdot \Delta t \tag{5}$$

where the index *"i"* may indicate reactant *B* or *C*.

In practice, after the average reaction rates stabilise their value, a macro time step Δt is performed by updating the concentration of the generic species *"i"* into the generic cell *"ic"* ($C_{i,ic}$) as follows:

$$\left(C_{i,ic}\right)_{t+\Delta t} = \left(C_{i,ic}\right)_t \cdot \frac{\left\langle C_i \right\rangle_{t+\Delta t}}{\left\langle C_i \right\rangle_t} \qquad (6)$$

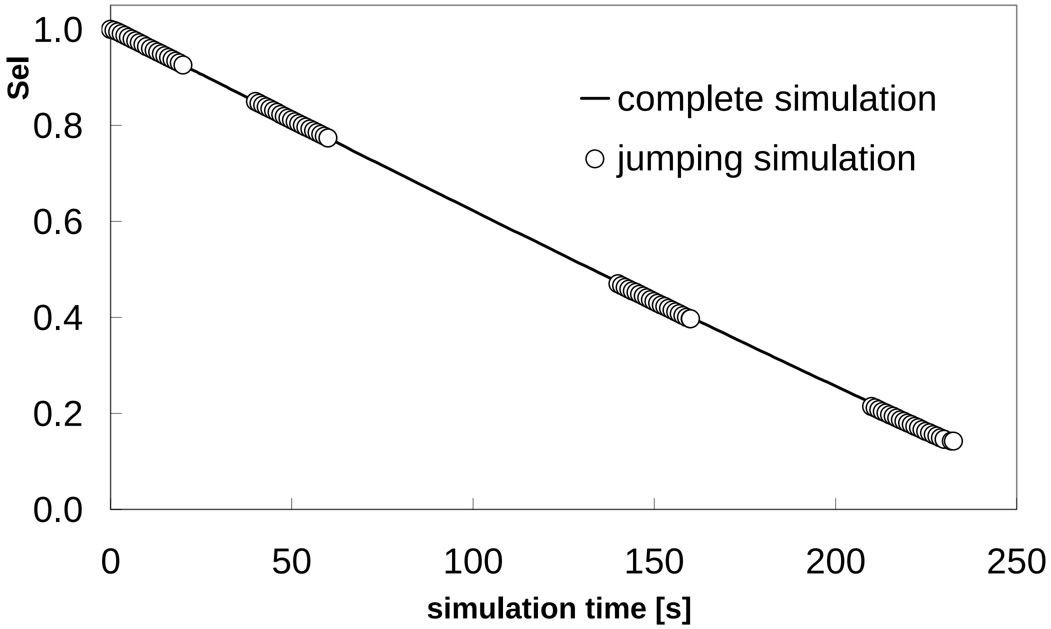

Fig. 3: Selectivity dynamics, comparison between full and "jumping" simulation results (T_{ini}=230 s, 400 rpm).

The common reactant concentration is updated according to the amount introduced during the macro interval and the amount consumed by the reactive processes.

In Figure 3 the average selectivity dynamics obtained by performing the simulation with the above described computational "jumping" technique is compared with the relevant value obtained by performing the complete simulation. The very good agreement observed clearly validates the technique, which was therefore used for all other simulations.

4. RESULTS AND DISCUSSION

Simulation results indicate that the reaction zone, *i.e.* the volume of the stirred tank where co-reactant *A* is consumed by the reactive processes, is confined to a relatively small region under the impeller near the injection point.

Each simulation was carried out until the entire amount of the co-reactant A had been consumed. The final selectivity towards reaction 2 was then computed according to Eq. 3.

Agitation speed effects on the selectivity for a given injection time (t_{inj}=230 s) are shown in Fig. 4. First of all it can be seen that the reported values are of the order of 10^{-1}, *i.e.* 7 orders of magnitude larger than in the case of a perfectly mixed system. As mixing intensity increases with agitation speed, a progressive reduction of selectivity is observed both for the experimental values and simulation results, as expected. As it can be seen the predicted selectivities are in good agreement with experimental results at all agitation speeds.

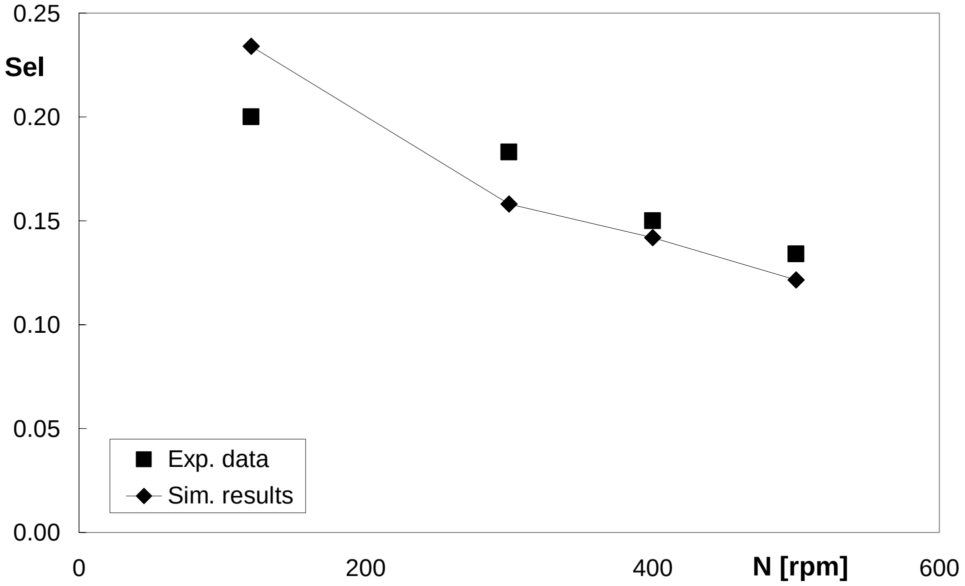

Fig. 4 – Selectivity *vs* agitation speed (T_{inj}=230 s).

The effect of reactant *A* injection time on the selectivity (for given agitation speed) is shown in Figs. 5 and 6, where simulation results (diamonds) are compared with experiment (solid squares) at two different agitation speeds. In both cases simulated selectivity values are in good agreement with the experimental data.

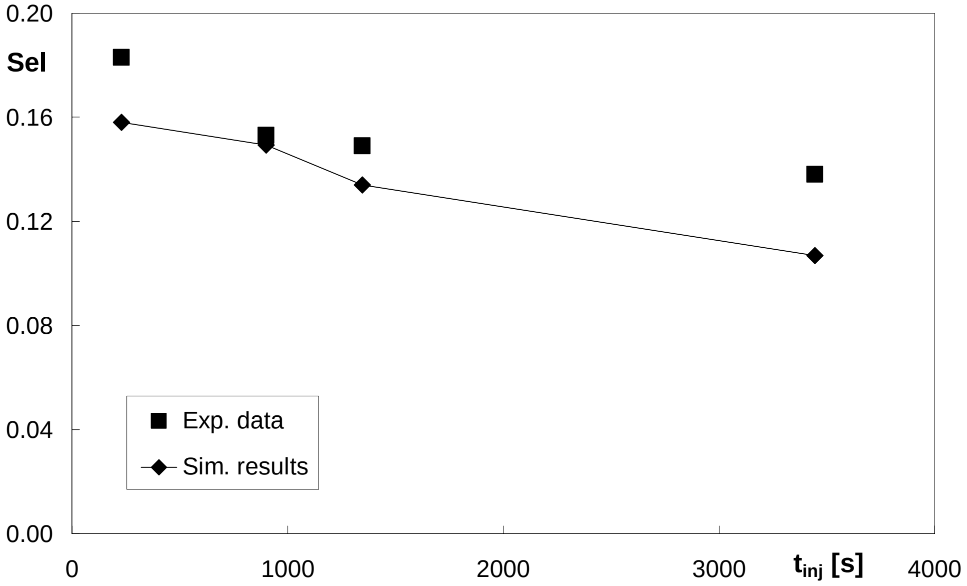

Fig. 5 – Selectivity *vs* injection time (N=300 rpm).

Interestingly, these results were obtained by taking into consideration only the “macro-mixing” phenomena in the tank, though the reaction pair employed practically coincided with that used in a number of works aimed at characterising “micro-mixing” phenomena (e.g. Rice & Baud, 1990; Thorma *et al.*, 1991; Baldyga *et al.,* 1997; Baldyga & Makowski, 2004).

A closer inspection of Figs. 5 and 6 indicate that there may be minor unresolved effects, possibly due to the micro-mixing phenomena overlooked in the simulations. In fact the predicted selectivities tend to progressively detach from the experimental values while injection time increases, as if the simulations tended to over predict the local mixing intensity. On the other hand, the discrepancies are limited to less than 25% (in the worst case), a figure that can be considered well within the acceptance level for design purposes.

It is finally worth noting that a fully predictive approach was applied here, with no adjustable parameters. It can be concluded that, for the reacting system here investigated, the macro-mixing plays the major role in determining the final concentration distribution of reactants and products. These findings confirm the similar results obtained by Brucato *et al.* (2000, 2002) where also no recourse to micro-mixing models was made in order to match simulations and experiments.

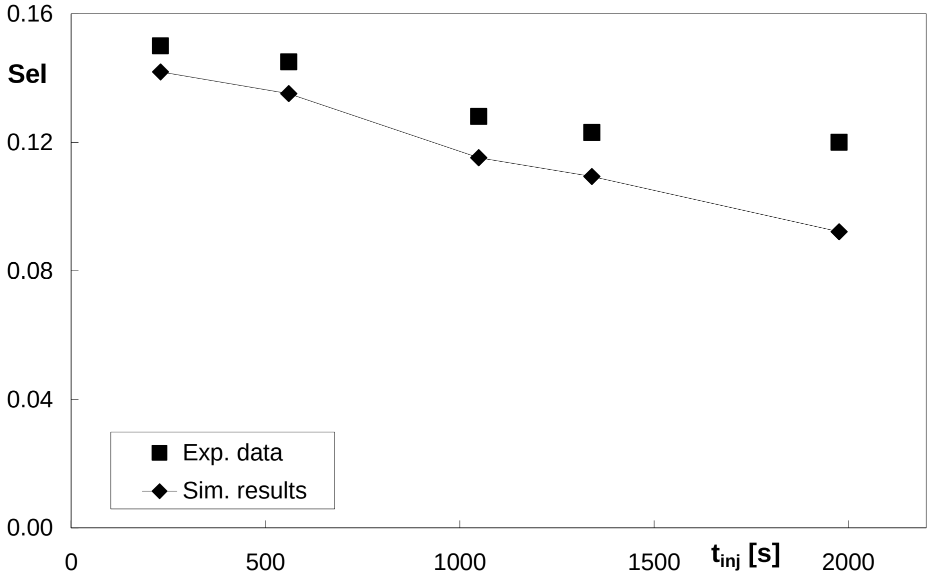

Fig. 6 – Selectivity *vs* injection time (N=400 rpm).

5. CONCLUSIONS

A CFD based fully predictive approach was developed to simulate the behaviour of a complex reactive system. Simulations concerned an unbaffled stirred vessel where a parallel-competitive reaction scheme was carried out in semi-batch conditions.

A computational technique was set up in order to speed up the reactive process simulations. In this way long lasting reactant injections could be simulated. The technique devised was validated by comparison with the standard (complete) computation.

The computed selectivities were found to agree well with experimental results, despite the many orders of magnitude difference with respect to perfect mixing predictions.

As the simulations were performed without considering any sub-grid (micro-mixing) model, it should be concluded that in the investigated case macro-mixing is the main factor affecting system behaviour. This findings extends the results previously obtained (Brucato *et al.* 2000, 2002) in the case of instantaneous injection and baffled vessels, to the case of unbaffled slowly-fed stirred reactors.

6. REFERENCES

Akiti, O., Arenante, P.M., 2004. Experimentally-validated micromixing-based CFD model for fed-batch stirred-tank reactors, AIChE Journal ,50 (3), 566-577.

Bakker, R.A., van den Akker, H.E.A., 1994. A computational study of chemical reactors on the basis of micromixing models, IChemE Symp. Series 136, 259-266.

Bakker, R.A., van den Akker, H.E.A., 1996. A lagrangian description of micromixing in a stirred tank reactor using 1D-micromixing models in a CFD flow field, Chemical Engineering Science, 51 (11), 2643-2648.

Baldyga, J., Bourne, J.R., 1990. The effect of micromixing on parallel reactions, Chemical Engineering Science, 45, 907-916.

Baldyga, J., Bourne, J.R., Hearn, S.J., 1997. Interaction between chemical reactions and mixing on various scales, Chemical Engineering Science, 52, 457-466.

Baldyga, J., Makowski, L., 2004. CFD Modelling of mixing effects on the course of parallel chemical reactions carried out in a stirred tank, Chemical Engineering and Technology, 27 (3), 225-231.

Bourne, J.R., Yu, S., 1991. An experimental study of micromixing using two parallel reactions. Proceedings of the 7th European Conference on Mixing, Brugge, Belgium, vol. I, 67–75.

Brucato, A., Ciofalo, M., Grisafi, F., Tocco, R., 2000. On the simulation of stirred tank reactors via computational fluid dynamics, Chemical Engineering Science, 55, 291-302.

Brucato, A., Grisafi, F., Micale, G., Rizzuti, L., 2002, “CFD simulation of stirred vessel reactors”, in Non Linear Dynamics and Control in Process Engineering, - Recent Advances (G. Continillo, S. Crescitelli, M. Giona editors), Springer Verlaag, 89-104.

Cotton, F.A., Wilkinson, G., 1988. Advanced inorganic chemistry. 53Ed., New York, Wiley.

Khang S. J., Levenspiel O., 1976. New scale-up and design methods for stirrer agitated batch mixing vessels, Chemical Engineering Science, 31, 569-577.

Middleton, J.C., Pierce, F., Lynch, P.M., 1986. Computations of flow fields and complex reaction yield in turbulent stirred reactors and comparison with experimental data, Chemical Engineering Research and Design, 64, 18-21.

Rice, R.W., Baud, R.E., 1990. The role of micromixing in the scale-up of geometrically similar batch reactors, A.I.Ch.E. Journal, 36 (2), 293-298.

Thorma, S., Ranade, V.V., Bourne J.R., 1991. Interaction between micro- and macro-mixing during reactions in agitated tanks, Canadian. Journal of Chemical Engineering, 69, 1135-1141.

Van De Vusse J.G., (1962), “A new model for stirred tank reactor”, Chemical Engineering Science, 17, 507-521.

ACKNOWLEDGEMENTS

This work was financially supported by the Ministry of Education, Roma (research project *FIRB 2001*, n° RBAU01NZH7). The authors are indebted to Marian Conigliaro and to Seraphine Saladino for their help in performing part of the work. The authors finally wish to thank CD-ADAPCO for kindly providing the software under special licence conditions.